



Oxidation of wastewater from TPA manufacturing process over carulite catalyst in sub- and supercritical water

Tae-Joon Park, Jong Sung Lim, Jae-Duck Kim,
Sung-Hyun Kim*, and Youn-Woo Lee
National Research Lab for Supercritical Fluid, KIST
Chemical Engineering Department, Korea University*

Introduction

Industrial wastewater treatment is one of the most important and urgent problems in environment management around the world. In particular, since a large amount of industrial wastewater of TPA process and polyester manufacture process come a significant environmental problem, to develop a management process for industrial wastewater of non-degradation organic compounds is of great importance.

The SCWO process produces environmentally acceptable effluents (gas, liquid, and solid), lends itself to resource recovery, and can be economically competitive. As such, the process can be used to serve as a pretreatment unit, as an end-of-pipe facility, or it can become an integral part of an industrial process. The aim of this study is to develop a SCWO process for destruction of wastewater came from TPA manufacturing plant and for recycle of process water. Generally, the wastewater is treated by aerobic wastewater treatment, followed by incineration of dried sludge.

We focus our attention on the use of supercritical water (SCW), which can dissolve hydrocarbons, expecting the control of product distribution and the decomposition effect of the wastewater. Therefore, the effect of temperature, pressure, oxidant amount, and reaction time on the decomposition of industrial wastewater from TPA manufacturing process was investigated

Experimental

The experiment apparatus was composed mainly of feed pump, wastewater storage, hydrogen peroxide storage, preheater, reactor, heat exchanger, filter, back pressure regulator, G/L separator and so on. This system was designed so that wastewater and hydrogen peroxide do not come in contact with each other until they have been pressurized and heated to the desired reaction conditions.

Each of the wastewater and the oxygen solution is heated in 1/16-in. OD x 4m length of SS 316 tube coiled in a preheater. The both streams were mixed at the reactor inlet. The reactor was made of stainless steel 316 (280mm long x 18mm OD x 9.5mm ID).

Results and Discussion

Eighty-seven oxidation experiments were performed for wastewater in an isothermal, isobaric packed bed flow reactor and all the experiments were carried out in the supercritical state. Carulite ($\text{MnO}_2/\text{Al}_2\text{O}_3/\text{CuO}$) was used as a catalyst in a tubular reactor. The reaction conditions ranged from pressures of 100 to 320bar, temperatures of 300 to 440 . The initial COD concentration of wastewater ranged from 53 to 1447 ppm (1.67 ~ 45.22 mmol/L).

The global rate for COD decomposition may be expressed as

$$\text{rate} = k[\text{COD}]^a[\text{H}_2\text{O}_2]^b[\text{H}_2\text{O}]^c \quad (1)$$

Equation (1) can be solved analytically with the initial condition $X=0$ at $W/F_{\text{COD}0}=0$ to provide equation (2) as the relationship between the COD composition conversion and the relevant process variables.

$$X = 1 - (1 - (1 - a)k(T)[\text{COD}]_0^a[\text{H}_2\text{O}_2]_0^b[\text{H}_2\text{O}]_0^c W / F_{\text{COD}0})^{1/(1-a)} \quad \text{if } a \neq 1 \quad (2)$$

We performed a non-linear regression analysis to fit the COD decomposition conversions. The hydrogen peroxide concentration is assumed constant throughout the reaction since H_2O_2 was always present in at least 200% excess of the stoichiometric requirement. Figure 1 shows a parity plot of the rate predicted from the global rate law using the parameters in Eq. (2) against the rate obtained experimentally by 31 data under critical temperature condition. The keys represent data at temperatures between 300°C and 360°C, these 31 data under critical temperature sets led to reaction orders of $a=1.09 (\pm 0.12)$ for COD, $b=0.09(\pm 0.07)$ for hydrogen peroxide, and $c=0.64 (\pm 1.56)$ for H_2O respectively.

The values of the Arrhenius parameters A and E_a are $9772.5(\pm 20712.0) \text{ mmol}^{-0.82}\text{s}^{-1}\text{L}^{1.82}\text{kg}^{-1}$ and $78.883(\pm 22.020) \text{ kJ/mol}$, respectively. The uncertainties reported here are the 95% confidence intervals, the sum of the squared residuals $(X_{\text{cal}} - X_{\text{exp}})^2$ was 0.0516.

Figure 2 shows a parity plot of the rate predicted from the global rate law using the parameters in Eq. (2) against the rate obtained experimentally by 56 data over critical temperature condition. The keys represent data at temperatures between 380°C and 440 , these 56 data over critical temperature sets led to reaction orders of $a=0.95 (\pm 0.05)$ for COD, $b=0.14(\pm 0.04)$ for hydrogen peroxide, and $c=-0.98 (\pm 0.07)$ for H_2O respectively. The values of the Arrhenius parameters A and E_a are $9037.8(\pm 7063.9) \text{ mmol}^{0.89}\text{s}^{-1}\text{L}^{0.11}\text{kg}^{-1}$ and $48.132(\pm 4.622) \text{ kJ/mol}$, respectively. The uncertainties reported here are the 95% confidence intervals, the sum of the squared residuals $(X_{\text{exp}} - X_{\text{cal}})^2$ was 0.0753.

Figure 3 shows overall parity plot of Figure 1 and Figure 2. The circle keys represent data at

temperatures between 300 and 360 , the square keys represent data at temperatures between 380 and 440 . The sum of the squared residuals $(X_{\text{exp}} - X_{\text{cal}})^2$ was that 0.0516 in Figure 1 added to 0.0753 in Figure 2 makes 0.1269.

Figure 4 shows parity plot of the rate predicted from the global rate law using the parameters in Eq. (2) and all data against the rate obtained experimentally without dividing temperature region. The keys represent data at temperatures between 300 and 440 , these 87 data sets led to reaction orders of $a=0.93 (\pm 0.05)$ for COD, $b=0.13 (\pm 0.03)$ for hydrogen peroxide, and $c=-0.97 (\pm 0.06)$ for H_2O respectively.

The values of the Arrhenius parameters A and E_a are $7528.4 (\pm 2154.1) \text{ mmol}^{0.91} \text{ s}^{-1} \text{ L}^{0.09} \text{ kg}^{-1}$ and $46.946 (\pm 1.940) \text{ kJ/mol}$, respectively. The uncertainties reported here are the 95% confidence intervals. The sum of the squared residuals $(X_{\text{exp}} - X_{\text{cal}})^2$ was 0.1476.

Acknowledgement

This work has been supported by the National Research Laboratory Program for Supercritical Fluid (2N21810) and the authors would like to thank to the Ministry of Science and Technology, Korea.

References

- T-J. Park, J. S. Lim, Y-W. Lee, S-H. Kim, Catalytic supercritical water oxidation of wastewater from terephthalic acid manufacturing process, *J. Supercritical Fluids*. (2002) In Press.
- J. Yu, P. E. Savage, Kinetics of Catalytic Supercritical Water Oxidation of Phenol over TiO_2 , *Environ. Sci. Technol*, 34 (2000) 3191.

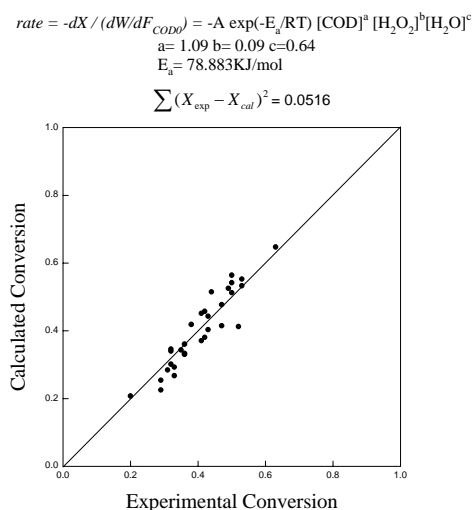


Figure 1. Parity plot for power-law equation using data under critical temperature region

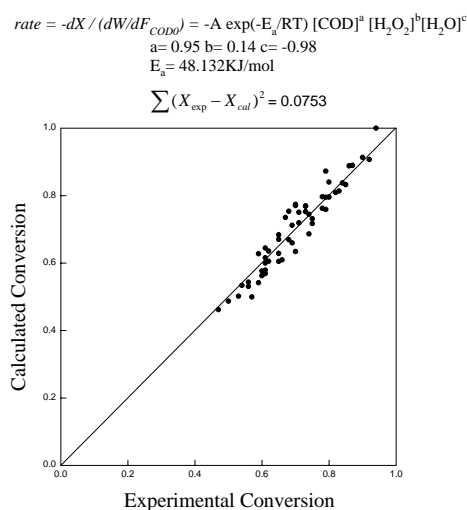


Figure 2. Parity plot for power-law equation using data over critical temperature region

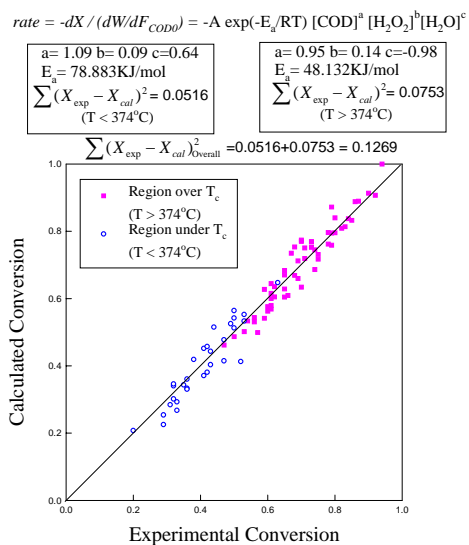


Figure 3. Overall parity plot for Figure 1 and Figure 2

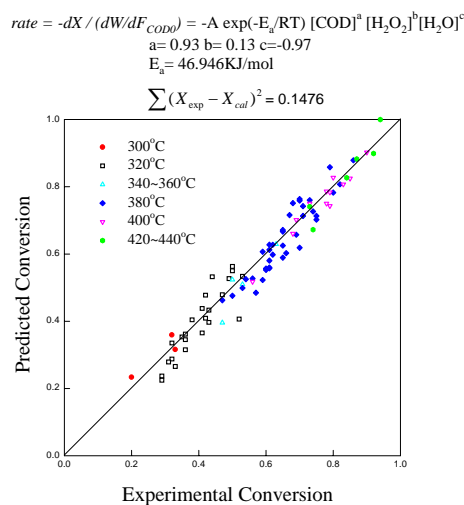


Figure 4. Parity plot for power-law rate equation using all data without dividing temperature region

A : rate = $-k[\text{COD}]^{0.95} [\text{H}_2\text{O}_2]^{0.14} [\text{H}_2\text{O}]^{-0.98}$ ($T > T_c$)
 B : rate = $-k[\text{COD}]^{1.09} [\text{H}_2\text{O}_2]^{0.09} [\text{H}_2\text{O}]^{0.64}$ ($T < T_c$)

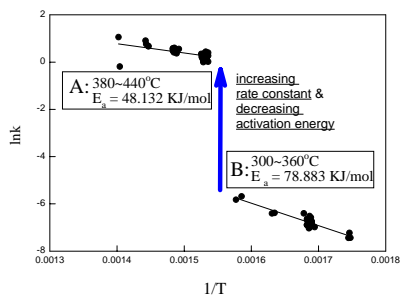


Figure 5. Arrhenius plot for wastewater oxidation by dividing temperature region

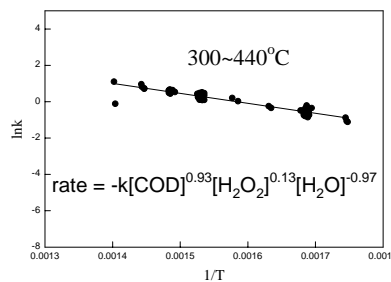


Figure 6. Arrhenius plot for wastewater oxidation in subcritical and supercritical water